

Climate–vegetation
modelling and fossil
plant data suggest
low atmospheric CO₂
in the late Miocene

M. Forrest et al.

Climate–vegetation modelling and fossil plant data suggest low atmospheric CO₂ in the late Miocene

M. Forrest^{1,*}, J. T. Eronen^{1,2,*}, T. Utescher^{1,3}, G. Knorr⁴, C. Stepanek⁴,
G. Lohmann⁴, and T. Hickler^{1,5,6}

¹Senckenberg Biodiversity and Climate Research Centre (BiK-F), Senckenberganlage 25, 60325 Frankfurt am Main, Germany

²Department of Geosciences and Geography, University of Helsinki, P.O. Box 64, 00014 Helsinki, Finland

³Steinmann Institute, University of Bonn, Nussallee 8, 53115 Bonn, Germany

⁴Alfred Wegener Institute, Bussestrasse 24, 27570 Bremerhaven, Germany

⁵Department of Physical Geography, Geosciences, Goethe University, Altenhöferallee 1, 60438, Frankfurt am Main, Germany

⁶Senckenberg Gesellschaft für Naturforschung, Senckenberganlage 25, 0325 Frankfurt am Main, Germany

*These authors contributed equally to this work.

Title Page

Abstract

Introduction

Conclusions

References

Tables

Figures

◀

▶

◀

▶

Back

Close

Full Screen / Esc

Printer-friendly Version

Interactive Discussion

Received: 5 May 2015 – Accepted: 17 May 2015 – Published: 16 June 2015

Correspondence to: J. T. Eronen (jussi.t.eronen@helsinki.fi)

Published by Copernicus Publications on behalf of the European Geosciences Union.

CPD

11, 2239–2279, 2015

Climate–vegetation modelling and fossil plant data suggest low atmospheric CO₂ in the late Miocene

M. Forrest et al.

[Title Page](#)

[Abstract](#)

[Introduction](#)

[Conclusions](#)

[References](#)

[Tables](#)

[Figures](#)



[Back](#)

[Close](#)

[Full Screen / Esc](#)

[Printer-friendly Version](#)

[Interactive Discussion](#)

Abstract

There is increasing need to understand the pre-Quaternary warm climates, how climate–vegetation interactions functioned in the past, and how we can use this information for understanding the present. Here we report vegetation modelling results for the Late Miocene (11–7 Ma) to study the mechanisms of vegetation dynamics and the role of different forcing factors that influence the spatial patterns of vegetation coverage. One of the key uncertainties is the atmospheric concentration of CO₂ during past climates. Estimates for the last 20 million years range from 280 to 500 ppm. We simulated Late Miocene vegetation using two plausible CO₂ concentrations, 280 and 450 ppm CO₂, with a dynamic global vegetation model (LPJ-GUESS) driven by climate input from a coupled AOGCM (Atmosphere–Ocean General Circulation Model). The simulated vegetation was compared to existing plant fossil data for the whole Northern Hemisphere. For the comparison we developed a novel approach that uses information of the relative dominance of different Plant Functional Types (PFTs) in the palaeobotanical data to provide a quantitative estimate of the agreement between the simulated and reconstructed vegetation. Based on this quantitative assessment we find that pre-industrial CO₂ levels are largely consistent with the presence of seasonal temperate forests in Europe (suggested by fossil data) and open vegetation in North America (suggested by multiple lines of evidence). This suggests that during the Late Miocene the CO₂ levels have been relatively low, or that other factors that are not included in the models maintained the seasonal temperate forests and open vegetation.

1 Introduction

The Late Miocene (11 to 7 Ma) belongs to the late phase of the Cenozoic climate cooling, during which the seasonality of climate in Europe intensified (e.g. Mosbrugger et al., 2005) and landscapes in North America opened (Eronen et al., 2012). In many regions, it was still characterised by warm and humid climatic conditions compared

CPD

11, 2239–2279, 2015

Climate–vegetation modelling and fossil plant data suggest low atmospheric CO₂ in the late Miocene

M. Forrest et al.

Title Page

Abstract

Introduction

Conclusions

References

Tables

Figures

◀

▶

◀

▶

Back

Close

Full Screen / Esc

Printer-friendly Version

Interactive Discussion

**Climate–vegetation
modelling and fossil
plant data suggest
low atmospheric CO₂
in the late Miocene**

M. Forrest et al.

[Title Page](#)[Abstract](#)[Introduction](#)[Conclusions](#)[References](#)[Tables](#)[Figures](#)[◀](#)[▶](#)[◀](#)[▶](#)[Back](#)[Close](#)[Full Screen / Esc](#)[Printer-friendly Version](#)[Interactive Discussion](#)

to today (Micheels et al., 2011; Utescher et al., 2011; Eronen et al., 2012; Fortelius et al., 2014). The global continental configuration in the Miocene was generally comparable to the modern situation with some small differences (e.g., Herold et al., 2008; Micheels et al., 2011). Marine evidence indicates that tropical sea surface temperatures were similar or even warmer than present in the Early to Middle Miocene (e.g., Stewart et al., 2004), and terrestrial equatorial regions were as warm as today in the Late Miocene (Williams et al., 2005; Steppuhn et al., 2006). The polar and Northern regions were warmer during the whole Miocene (e.g., Wolfe, 1994a, b; Utescher et al., 2011; Popova et al., 2012). Similarly, the North Pacific in the Late Miocene was warmer than today (Lyle et al., 2008). CO₂ levels during the Late Miocene can still not be reconstructed with certainty (see e.g. discussion in Beerling and Royer, 2011): estimates for the atmospheric CO₂ levels range from 280 ppm to as high as 500 ppm. Recent studies suggest about 350–500 ppm for the Middle Miocene (Kürschner et al., 2008; Foster et al., 2012; Zhang et al., 2013), and around 280–350 ppm for the Late Miocene (Zhang et al., 2013, their Fig. 5). In addition, terrestrial proxy data suggest that during the Late Miocene there was a marked increase in both temperature and precipitation seasonality (Janis et al., 2002; Mosbrugger et al., 2005; Eronen et al., 2010, 2012). Plant-based data evidence that the increase in temperature seasonality was mainly effective in the middle to higher latitudes (Utescher et al., 2011), while the evolution of precipitation seasonality was strongly region-dependant and variable throughout the late Miocene (Syabryaj et al., 2007; Utescher et al., 2015). Knorr et al. (2011) modelled the impact of vegetation and tectonic conditions on the Late Miocene climate, and showed that the vegetation has a considerable effect on the climate, and that Late Miocene warmth can be modelled with relatively low CO₂ concentrations at pre-industrial level (278 ppmv). Further, LaRiviere et al. (2012) showed that the oceanic state in the Late Miocene was similar to that of Early Pliocene, with a deeper thermocline, high SSTs, and low SST gradients. They further suggested that, based on their data, during the Late Miocene and earlier times, CO₂ and oceanic warmth were decoupled because of deeper thermoclines. The tight link between ocean temperature and CO₂ formed only during the

Climate–vegetation modelling and fossil plant data suggest low atmospheric CO₂ in the late Miocene

M. Forrest et al.

[Title Page](#)

[Abstract](#)

[Introduction](#)

[Conclusions](#)

[References](#)

[Tables](#)

[Figures](#)

[◀](#)

[▶](#)

[◀](#)

[▶](#)

[Back](#)

[Close](#)

[Full Screen / Esc](#)

[Printer-friendly Version](#)

[Interactive Discussion](#)

Pliocene when the thermocline shoals and surface water became more sensitive to CO₂. Bolton and Stoll (2013) on the other hand suggested that, based on coccolith data analysis, the atmospheric CO₂ concentration decreased during the latest Miocene (7–5 Ma). They also suggested that atmospheric CO₂ content might have been higher (400–500 ppm, based on Zhang et al., 2013) during the Middle and Late Miocene, and that the substantial ocean surface cooling during the last 15 Ma may reflect the global decrease in the CO₂ concentration.

The Late Miocene is a sub-epoch of the Miocene, which is generally dated roughly between 11 to 5 million years. It includes the Tortonian and Messinian stages. The climate and vegetation models we use in this study use the boundary conditions specific for the Tortonian. The Tortonian comprises the time-interval between 11.6 and 7.2 Ma (Gradstein et al., 2004). It corresponds roughly to European mammal units MN9 to MN12, and Vallesian and lower Turolian mammal zones (Steininger, 1999). The boundary conditions used for the climate model, as well as the proxy data we use, are dated within these time slices. From here on, we just use the term Tortonian to indicate this time period, and refer to the Late Miocene when we discuss trends in more general terms.

Here we run the dynamic global vegetation model (DGVM) LPJ-GUESS (Smith et al., 2001; Sitch et al., 2003; Ahlström et al., 2012) for the Tortonian with two different CO₂ concentrations to investigate the vegetation dynamics during this period. We use climate data simulated for the Tortonian by Knorr et al. (2011) and Knorr and Lohmann (2014), using a fully coupled AOGCM without any flux corrections. We concentrate on whether the DGVM can create and maintain the mid-latitude seasonal vegetation cover in a generally warmer world, as suggested by the proxy data, and on the sensitivity of the vegetation to CO₂ concentration. We compare our results with existing terrestrial proxy data and previous modelling results, and discuss the implications from our results. Our hypothesis is that in order to maintain the seasonal and open vegetation of the Late Miocene, we need low atmospheric CO₂ concentration.

2 Previous model studies

Several vegetation model runs have been performed previously for the Late Miocene period. One of the first was a BIOME4 model (Kaplan, 2001) run for the Tortonian by Micheels (2003) to interpolate between the vegetation reconstructed by qualitative interpretation of proxy data from palaeobotanical literature. In this reconstruction the tropical forests expand in the Tortonian, and their margins shift further poleward. Much of Africa was generally characterised by tropical forest vegetation. Accordingly, the Sahara desert was smaller than today and consisted of steppe and open grassland, rather than sand desert. Woodier Tortonian vegetation replaced the present-day's warm-arid desert, semi-desert and grassland regions.

Francois et al. (2006) used the CARAIB model together with the ECHAM4/ML AOGCM to reconstruct the distribution of vegetation and carbon stocks during the Tortonian (7–11 Ma) with different CO₂ levels. The main difference to our model setup is that ECHAM4 was not coupled to a dynamic ocean model, but a mixed layer ocean model. Their Tortonian run with 280 ppm CO₂ showed a general trend of reduction of desert areas worldwide and appearance of tropical seasonal forests in the warm temperate zone of the Northern Hemisphere, between 30 and 50° (Fig. 4 of Francois et al., 2006). With their 560 ppm CO₂, most deserts disappeared from the continental surface, except for the Sahara. The extent of tropical seasonal forests also appeared to be extremely sensitive to the atmospheric CO₂ level. Francois et al. (2011) further used the CARAIB model to study the Tortonian vegetation in Europe in detail. On average, their standard 280 ppm run is too cool, with too few temperate humid evergreen trees in Southern Europe compared to their proxy data. Also other models (see below) have struggled to reproduce the seasonal forests in Europe that are known to have existed for the last 10 million years (e.g. Agusti et al., 2003; Mosbrugger et al., 2005).

Pound et al. (2011) used BIOME4, driven by the HadAM3 atmosphere-only general circulation model, and palaeobotanical proxies to create an advanced global data-model hybrid biome reconstruction for the Tortonian. In their runs boreal forests reach

CPD

11, 2239–2279, 2015

Climate–vegetation modelling and fossil plant data suggest low atmospheric CO₂ in the late Miocene

M. Forrest et al.

Title Page

Abstract

Introduction

Conclusions

References

Tables

Figures

◀

▶

◀

▶

Back

Close

Full Screen / Esc

Printer-friendly Version

Interactive Discussion

Climate–vegetation modelling and fossil plant data suggest low atmospheric CO₂ in the late Miocene

M. Forrest et al.

[Title Page](#)

[Abstract](#)

[Introduction](#)

[Conclusions](#)

[References](#)

[Tables](#)

[Figures](#)

[◀](#)

[▶](#)

[◀](#)

[▶](#)

[Back](#)

[Close](#)

[Full Screen / Esc](#)

[Printer-friendly Version](#)

[Interactive Discussion](#)



80° N, and temperate forests were present north of 60° N. Warm-temperate forests cover most of Europe, North America and South-East Asia. There is temperate savannah in central USA. Most areas that are deserts today are covered by grasslands and woodlands in their run. The extent of tropical forests in South America was reduced. Scheiter et al. (2012) used the adaptive DGVM (aDGVM) forced with climate data from HadCM3L and carried out factorial vegetation model runs to investigate the role of fire, emergence of C₄ photosynthesis, and atmospheric CO₂ levels in the vegetation dynamics of Africa. In their runs, vegetation openness is mainly determined by fire; generally too much forest cover is simulated if fire disturbance is switched off. The biome patterns are relatively insensitive to both changes in the CO₂ concentration or the introduction of herbaceous vegetation with C₄ photosynthesis.

3 Methods

3.1 Palaeoclimate simulations

The climate simulations have been performed with an AOGCM. The atmosphere model component ECHAM5 (Roeckner et al., 2003) was used at T31 resolution ($\sim 3.75^\circ$) with 19 vertical levels. The ocean model MPIOM (Marsland et al., 2003) was run with a bipolar curvilinear GR30 resolution ($\sim 3^\circ \times 1.8^\circ$) with 40 vertical layers. This modelling approach has been evaluated with proxy data in investigations of the Tortonian (Micheels et al., 2011; Knorr et al., 2011) and the Middle Miocene climate transition (Knorr and Lohmann, 2014). We used the same boundary conditions as Micheels et al. (2011) with respect to the tectonic setting and the vegetation distribution. We applied minor land–sea modifications, as described in Knorr et al. (2011), e.g., a closed Hudson Bay (Smith et al., 1994). We used data from two model runs with different CO₂ settings, one with a lower CO₂ concentration of 278 ppm (after this referred to as “280 ppm run”, from Knorr et al., 2011) and one with a higher CO₂ concentration of 450 ppm (after this referred to as “450 ppm run”, from Knorr and Lohmann, 2014).

For further details of the AOGCM model configuration and the boundary conditions we refer the reader to Micheels et al. (2007, 2011), Knorr et al. (2011), and Knorr and Lohmann (2014).

3.2 Correction of present-day biases in climate simulations

To correct for biases in climate simulations, the difference between the Tortonian climate simulations and the pre-industrial control simulation in Knorr et al. (2011) (the Control) was applied to present day climate data to form the palaeoclimate. The Princeton Global Forcing dataset (PGF, Sheffield et al., 2006) was selected as the present day climate baseline. This dataset is a reanalysis product (produced by running an atmospheric circulation model with data assimilation using meteorological measurements) and has been bias-corrected using ground and satellite observations of meteorological variables. Thus it provides global data on a daily or sub-daily time-step which has been dynamically interpolated from station measurements and, by using observed meteorological measurements, is corrected for biases originating from the atmospheric circulation model.

The palaeoclimate anomalies were calculated using the mean values from 100 years of climate simulation and applied following the approach of François et al. (1998) but on a daily, rather than a monthly, time step. The years 1951–1980 were selected to represent the pre-industrial climate, as they give a reasonable compromise between the need for low atmospheric CO₂ (to better represent pre-industrial climate) and the need for maximal instrumentation to measure the climate and so better constrain the atmospheric circulation model.

3.3 Vegetation simulations

The palaeoclimate model results were used to drive the DGVM LPJ-GUESS. The soil texture map used in the vegetation simulations was derived by translating the soil texture map used by the palaeoclimate AOGCM simulations to the soil classes detailed

Climate–vegetation modelling and fossil plant data suggest low atmospheric CO₂ in the late Miocene

M. Forrest et al.

Title Page

Abstract

Introduction

Conclusions

References

Tables

Figures

◀

▶

◀

▶

Back

Close

Full Screen / Esc

Printer-friendly Version

Interactive Discussion



Climate–vegetation modelling and fossil plant data suggest low atmospheric CO₂ in the late Miocene

M. Forrest et al.

[Title Page](#)

[Abstract](#)

[Introduction](#)

[Conclusions](#)

[References](#)

[Tables](#)

[Figures](#)

[◀](#)

[▶](#)

[◀](#)

[▶](#)

[Back](#)

[Close](#)

[Full Screen / Esc](#)

[Printer-friendly Version](#)

[Interactive Discussion](#)

in Sitch et al. (2003). The representation of vegetation in the palaeoclimate AOGCM comprised statically prescribed land surface classes from Micheels (2003) and as such cannot vary to reach equilibrium with the climate. By using a DGVM with offline climate data we allow the vegetation to reach equilibrium with the (now static) climate. This forms the first step of an asymmetric, iterative offline coupling. Thus we consider our vegetation map to be an iteratively improved version of the original land-cover map of Micheels (2003), improved in the sense that it has undergone one cycle of simulated climate-land surface feedbacks, and has used a more fully developed DGVM with more detailed process representations.

LPJ-GUESS (Smith et al., 2001) combines the generalized representations of the physiological and biophysical processes embedded in the widely used global model LPJ-DGVM (Sitch et al., 2003) with detailed representations of tree population dynamics, resource competition and canopy structure, as generally used in forest gap models (Bugmann, 2001; Hickler et al., 2004). Here, we build upon a recent version, including a representation of wildfires (Thonicke et al., 2001), the hydrology scheme from Gerten et al. (2004), and updates, in particular concerning the Plant Functional Type (PFT) parameterization, described by Ahlström et al. (2012). The bioclimatic limits from Ahlström et al. (2012) were revisited and modified, as described below. The new bioclimatic limit parameterizations improve the simulated present-day vegetation compared to an independently derived expert map. In our version, the bioclimatic limits follow the original values in Sitch et al. (2003). The boreal/temperate shade-intolerant summergreen broadleaved tree (IBS) PFT in Ahlström et al. (2012) was split into separate boreal and temperate PFTs with temperature limits on photosynthesis, as the other boreal and temperate PFTs, respectively. The base respiration rates of boreal PFTs were increased compared to temperate trees (as in Hickler et al., 2012), reflecting the general increase of base respiration rates with decreasing temperature (Lavigne and Ryan, 1997). Finally, a Temperate Needle-leaved Evergreen PFT (TeNE) was added based on a similar PFT in Sitch et al. (2003). Note that the C₃ and C₄ grass PFTs include forbs, not only grasses. In this paper we refer to these PFTs as grasses because

grasses comprise most of the biomass of these PFTs, and this term is more consistent with the terminology used in the palaeobotanical reconstructions. A full list of PFTs and parameter values is given in Appendix A.

The fire model GlobFIRM (Thonicke et al., 2001) with an updated parameterisation as described in Pachzelt et al. (2015), but applied globally, was used to simulate wildfires. Representation of fire processes is important when studying vegetation dynamics and structure, particular when considering landscape openness.

We performed a biomisation (based on Hickler et al. (2006) but with small changes, see Appendix B) to visualise the simulated Tortonian vegetation (Fig. 1a and c), and to compare the vegetation simulation of the present day to a present-day biome map (Fig. S1 in the Supplement). The pre-industrial control run (Knorr et al., 2011) reproduced the modern biomes (Fig. S1a) reasonably well.

3.4 Statistics to compare modelled and fossil vegetation

Quantitative comparisons of fossil data and model output are challenging. As described below, the palaeobotanical record provides the presence of fossil taxa at a given site and each taxon is then assigned to a PFT. The final values for each site are therefore the number of taxa assigned to each PFT. This is a measure of PFT *diversity*, but typically it is PFT *abundances* which are used to describe vegetation and biomes on a global scale, and it is these quantities which are provided by vegetation models. There are various difficulties when attempting to draw conclusions from comparisons between diversity data from the fossil record and modelled abundances or biomes. Firstly, abundances and diversity are not necessarily closely correlated; some PFTs might have few taxa but massive abundance (for example Boreal Needle-leaved Trees). Secondly, the fossil record has biases; some PFTs fossilise at higher rates than others, and time-dependent climate fluctuations (Milankovic cycles and the formation and destruction of microclimates) may make the fossil record unrepresentative of PFT diversities over the whole time period. A further problem is that it is difficult to know how PFT diversities in the fossil record correlate to an abundance measure that can be simulated by a veg-

Climate–vegetation modelling and fossil plant data suggest low atmospheric CO₂ in the late Miocene

M. Forrest et al.

Title Page

Abstract

Introduction

Conclusions

References

Tables

Figures

◀

▶

◀

▶

Back

Close

Full Screen / Esc

Printer-friendly Version

Interactive Discussion



Climate–vegetation modelling and fossil plant data suggest low atmospheric CO₂ in the late Miocene

M. Forrest et al.

[Title Page](#)

[Abstract](#)

[Introduction](#)

[Conclusions](#)

[References](#)

[Tables](#)

[Figures](#)



[Back](#)

[Close](#)

[Full Screen / Esc](#)

[Printer-friendly Version](#)

[Interactive Discussion](#)



etation model. An example of a commonly used abundance measure from vegetation models is Leaf Area Index (LAI), the leaf area per unit ground area. Standard statistical tests, such as goodness of fit between modelled PFT LAI fraction and the PFT diversities in the fossil record, did not yield useful results (data not shown), possibly for the reasons discussed above.

To go beyond simple visual comparisons of model and data, and for hypothesis testing, we require a quantitative measure of agreement between fossil data and model output. Different approaches have been developed to compare fossil data to model results with some quantitative element. The approach taken in Salzmann et al. (2008) and Pound et al. (2011) involves classifying both the fossil data and the model output into biomes, which necessarily require subjective choices. Francois et al. (2011) compared on a PFT level and provided a per-PFT percentage agreement across sites based only on presence/absence. Neither approach offers a single summary statistic on the interval scale that can be compared between scenarios for hypothesis testing. We prefer a metric that uses only the raw data without a biome classification, using more information than provided by presence-absence data, and providing a simple number to summarise overall agreement for a given model run.

To this end we developed an Agreement Index (AI). This index takes into account all the fractional representations of different PFTs in the model (LAI) and fossil data (number of taxa) for each fossil site. A PFT can have one of 4 statuses in a gridcell in both the fossil data and the model output. These statuses are [fossil, model]: (1) dominant – fraction in the range (0.50, 1.0], (2) sub-dominant – fraction in the range (0.15, 0.50], (3) trace – fraction in the range (0.05, 0.15], (4) absent – [0, 0.05]. These are then compared between fossil and model for each PFT, and a contribution quantifying the degree of agreement is added to the AI for the gridcell as given in Table 1. The AI is then averaged across all fossil sites.

The logic of the AI is as follows. If a PFT is absent in both the data and the model it contributes 0, since correctly not simulating a PFT is not much of a test of model skill. This also has the desirable effect that a PFT, which is only minimally represented in both

Climate–vegetation modelling and fossil plant data suggest low atmospheric CO₂ in the late Miocene

M. Forrest et al.

[Title Page](#)

[Abstract](#)

[Introduction](#)

[Conclusions](#)

[References](#)

[Tables](#)

[Figures](#)

[◀](#)

[▶](#)

[◀](#)

[▶](#)

[Back](#)

[Close](#)

[Full Screen / Esc](#)

[Printer-friendly Version](#)

[Interactive Discussion](#)

the fossil record and the model output, does not strongly affect the final AI value. If the PFT status matches between the model and the data, then it contributes +1, except if it is the dominant PFT, in which case +2 is added. The dominant PFT is weighted more heavily because it defines the biome and represents the most significant component of the vegetation present. If the model and data mismatch by one category (e.g. the PFT is trace in the model but absent in the data, or dominant in the data but only sub-dominant in the model) then there is a contribution of 0. In such a case the model is not exactly right, but it is not too far away. Given the large uncertainties in inferring relative abundance from fossil diversity data, this degree of statistical mismatch is acceptable. If the data and model differ by two categories (say, the PFT is sub-dominant in the model but absent in the data) this represents a mismatch and contributes −1. Finally, if model and data mismatch by three categories (cases where a PFT is absent in the data but dominant in the model, or vice-versa) a contribution of −2 is added to the AI as this indicates large data-model disagreement.

The range of possible values that the AI can take at a given site is determined by the composition of fossil PFTs at the site. Averaging across all sites used in this analysis gives a range of (−11.4, 4.7). However, this range is relatively meaningless as the chances of getting perfect agreement or perfect disagreement are vanishingly small. In order to simulate the level of agreement that might be expected simply by chance, a set of 25 000 AI values were produced by matching each fossil sites to a randomly selected gridcell chosen from the 280 and 450 ppm model runs combined. This gives an approximate null model with an expectation value for chance agreement and a standard deviation to test for significance. The expectation value was −1.96 (close to the centre point of the theoretically possible range) with a standard deviation of 0.17. We suggest this approach as a robust and quantitative comparison of similar model setups for hypothesis testing, as well as a general measure of agreement between fossil data and simulation results.

3.5 Palaeobotanical data

The plant data we used are taken from the NECLIME data set as published in the PAN-GAEA database (doi:10.1594/PANGAEA), completed by data from the authors (full list of sites is provided in Supplement). After removing sites with more than 20 % aquatic taxa, representing azonal sites (not by macroclimate but by local topographic features determined vegetation, such as riparian vegetation, which is not represented by the vegetation model), the set comprised a total of 167 macro (fruits and seeds, leaves) and micro (pollen/spores) floras, dated to the Late Miocene (11–7 Ma). To assign PFTs to the fossil plant record, we classified the Nearest Living Relatives of the fossil plant taxa in terms of PFT types that are used in LPJ-GUESS (see Table S1 in Supplement). Depending on ecological amplitude of a taxonomic unit and the achievable taxonomic resolution, respectively, a single fossil taxon may represent various different PFTs. Therefore, a matrix containing modern taxa and PFT scores was first established, with PFT scores for each taxon adding up to 1. Diversities of PFTs were then calculated for all sites by using a matrix with taxa records together with a matrix containing the scores of the represented PFTs. Taxa diversity in the considered floras is highly variable, ranging from 7 to 129, and the floral data set is heterogeneous regarding its representativeness with respect to PFTs and the spatial scales at which palaeovegetation is mirrored (Utescher et al., 2007). Pollen floras usually allow characterizing regional vegetation, while leaves involve a local signal. Regarding the representativeness of fossil data with respect to PFTs, leaf floras reflect arboreal PFTs well, while remnants of herbaceous PFTs and grasses are rarely preserved. In pollen floras, on the other hand, the herbaceous vegetation tends to be over-represented while fruit and seed floras may be biased regarding the richness of aquatics. With all these uncertainties, we decided to use all palaeofloras for maximal geographic coverage, excluding aquatic ones, dated to the studied time slice.

Various PFTs present in the fossil record, such as forbs, shrubs, lianas, tuft trees, aquatics, etc., are not considered in the analysis because they do not have any cor-

Climate–vegetation modelling and fossil plant data suggest low atmospheric CO₂ in the late Miocene

M. Forrest et al.

Title Page

Abstract

Introduction

Conclusions

References

Tables

Figures



Back

Close

Full Screen / Esc

Printer-friendly Version

Interactive Discussion

Climate–vegetation modelling and fossil plant data suggest low atmospheric CO₂ in the late Miocene

M. Forrest et al.

[Title Page](#)

[Abstract](#)

[Introduction](#)

[Conclusions](#)

[References](#)

[Tables](#)

[Figures](#)

[⏪](#)

[⏩](#)

[◀](#)

[▶](#)

[Back](#)

[Close](#)

[Full Screen / Esc](#)

[Printer-friendly Version](#)

[Interactive Discussion](#)

and Rocky mountain area of North America are more open than in the 450 ppm run, and C₃ grasses are the dominant PFT over a much larger area (Fig. 1a and b). Another region of interest is Europe, because of its high density of palaeobotanical proxy data. Whilst both runs show Europe to be mostly forested, with the expected northwards shift of biome boundaries compared to the present day, the 280 ppm run shows more deciduous vegetation in Central Europe and more open vegetation in the south which agrees better with European proxy data. These results are discussed further below.

One feature that is very different between our model-based reconstructions, and also between different vegetation and climate models, is the vegetation of Greenland (e.g. Francois et al., 2006; Pound et al., 2011, our results). In most cases, Greenland is assumed to be largely covered with taiga and cold deciduous forests instead of the present-day's ice cover, but there are no fossil data to confirm this. Another large-scale feature of note is that the modern-day Sahara region is vegetated with dry grasslands.

4.2 Comparison of 280 and 450 ppm simulations

Our simulation results with both CO₂ concentrations correspond well with other vegetation modelling and reconstruction results (e.g. Francois et al., 2006, 2011; Pound et al., 2011) and the palaeobotanical data. Using our quantitative approach, we see that the 280 ppm run shows better agreement with palaeobotanical data than the 450 ppm run. Specifically, the 450 ppm reconstruction yields an AI value of -0.97 , and a Z score of 5.8 , whereas the 280 ppm reconstruction shows better agreement with an AI value of -0.67 , and a Z score of 7.5 (Fig. 2).

In order to disentangle the indirect effect of CO₂ on vegetation via climate, and the direct effect of CO₂ on vegetation, we performed additional simulations with 450 ppm CO₂ in the vegetation model with the 280 ppm CO₂ climate model results and vice versa. The vegetation results with 450 ppm climate and 280 ppm vegetation have the worst agreement, with an AI score of -1.02 . The run with 280 ppm climate and 450 ppm vegetation yields an AI of -0.60 , which is slightly better than the full 280 ppm run. AI scores with the same CO₂ in the climate but different CO₂ in the vegetation are simi-

lar, whereas AI scores with different CO₂ in climate but identical CO₂ in the vegetation are more dissimilar (Table 2). This strongly suggests that climate CO₂ is the dominant effect in our simulations.

We see that with 280 ppm in the climate there are more open conditions in North America, regardless of the vegetation CO₂ (Figs. 1, 3 and 4). This is strongly supported by fossil mammal and phytolith data (see below). In Central Europe, the tendency towards more deciduous vegetation is also driven by low CO₂ in the climate, not low CO₂ in the vegetation, shown by the Central European AI values in Table 3. In other areas the patterns are less clear. In tropical regions, the direct effect of CO₂ on vegetation is stronger than the effect via climate, possible because in these areas temperature and precipitation is not limiting. In cooler areas (in particular the boreal zone), the effect of CO₂ in the climate system of increasing temperatures is stronger than the CO₂ fertilisation effect on vegetation, since these areas are temperature limited.

The result that 280 ppm run agrees better with the palaeobotanical data poses a question: how can we have the combinations of moderately low CO₂, seasonal mid-latitude conditions, a generally warmer world, and shallower latitudinal temperature gradient at the same time? Generally, so far the answer has been that the CO₂ concentration must have been higher in the past to create the Late Miocene warmth (see introduction). However, there has been increasing evidence that atmospheric CO₂ during the Late Miocene has not been much higher than during pre-industrial times (e.g. Pearson and Palmer, 2000; Beerling and Royer, 2011; Zhang et al., 2013). This remains an open question, but it is outside the scope of the present study.

To check the consistency of the result with respect to the choice of the boundaries between the agreement index statuses, these boundaries were varied in an a posteriori systematic study. A full factorial approach was taken and the boundaries were varied from 50 up to 200 % of their initial values. It was found that the magnitude of AI values were sensitive to the boundaries chosen (varying between about -2 and 1), but that the 280 ppm reconstruction gave a consistently higher AI values than the 450 ppm

CPD

11, 2239–2279, 2015

Climate–vegetation modelling and fossil plant data suggest low atmospheric CO₂ in the late Miocene

M. Forrest et al.

Title Page

Abstract

Introduction

Conclusions

References

Tables

Figures



Back

Close

Full Screen / Esc

Printer-friendly Version

Interactive Discussion

Climate–vegetation modelling and fossil plant data suggest low atmospheric CO₂ in the late Miocene

M. Forrest et al.

[Title Page](#)

[Abstract](#)

[Introduction](#)

[Conclusions](#)

[References](#)

[Tables](#)

[Figures](#)



[Back](#)

[Close](#)

[Full Screen / Esc](#)

[Printer-friendly Version](#)

[Interactive Discussion](#)



Central Europe compared to the 280 ppm run. The Mediterranean is still a mix of grasslands, savannas and forests, but with a tendency towards the woodier biome types and an increase in temperature evergreen trees (Fig. 1).

When comparing to other reconstructions and palaeobotanical data it should be noted that, based on proxy data, the late Miocene vegetation in the lower latitudes of Europe has been characterized as Mixed Mesophytic Forest, an association of thermophilous broadleaved summergreens and conifers as canopy trees, with variably diverse evergreen woods in the understory (Utescher et al., 2007). This characteristic type, however, cannot be resolved in the biome system we presently use.

The Pound et al. (2011) BIOME4 simulation produces tropical xerophytic shrublands for Western and Southern Europe. This is a drier vegetation type than the fossil data, and different from our model run. For Central Europe, the BIOME4 simulation exhibits warm mixed forests, this agrees well with data and our simulations. The simulations also agree in that the boreal forests are confined to the extreme north of Europe.

The 200/280 ppm global simulations of Francois et al. (2006) produce vegetation in Europe which is very similar to the present day, whereas the 560 ppm run produces tropical seasonal forests in Europe. The presence of tropical seasonal forests in Europe is not well-supported by palaeobotanical proxy data. All of their simulations show a greater extent of the boreal forest than in either in Pound et al. (2011) or our simulations.

In the higher resolution, regional study of Francois et al. (2011), most of Europe is dominated by cool-temperate mixed and temperate broadleaved deciduous forests, but there is presence of warmer vegetation types around the Adriatic Sea and in the north of Turkey. Warm-temperate mixed forests grow around the western part of the Paratethys, and an extension of the tropical grassland around the Mediterranean Sea can be observed. These latter aspects are similar to our simulations.

4.3.2 North America

Our 280 ppm model run exhibits vegetation that is similar to the present day in North America. Compared to the 450 ppm runs, this vegetation is more open and seasonal in the Great Plains and Rocky Mountains. The openness is apparent from the increase of C₃ grass PFT dominance, and from the reduction of tree cover and the corresponding savanna classification in the biome plots (Figs. 1c and d, 3 and 4). The increased seasonality is shown by the reduction in dominance of the temperate broadleaved evergreen PFT, and by the increase of C₃ grass at the expense of trees. Whilst there are few fossil data points in North America, other available data from isotopes (Passey et al., 2002), mammalian community structure (Janis et al., 2004), mammal-based precipitation estimates (Eronen et al., 2012), as well as phytoliths (Strömberg, 2005) support the open landscapes and graze-dominated faunas during the Tortonian in the Great Plains, as do both midland plant localities in our record (sites Kilgore, Antelope; C₃ PFT diversity fraction 20, 60 %). In addition, the data presented in Pound et al. (2011) indicate more open and seasonal vegetation in this region during the Tortonian. In light of these sources of evidence, it appears that the 280 ppm simulation reproduces the vegetation of the central North America considerably better than the 450 ppm simulation. The importance of low CO₂ for maintaining open landscapes has also been suggested by other modelling studies. Harrison and Prentice (2003), for example, found that the BIOME4 vegetation models consistently overestimated glacial tree cover, if physiological effects of low atmospheric CO₂ were not accounted for. Experimental elevation of CO₂ above ambient levels has been shown to promote shrub encroachment into steppes (Morgan et al., 2007).

A further notable difference is that the 450 ppm simulation exhibits a strong northward movement of biome boundaries compared to the 280 ppm run, which are indicative of a considerably warmer and wetter climate (Fig. 1a and b). There is a northward shift of the boreal/temperate boundary in the 450 ppm run compared to the 280 ppm run. Temperate forests have larger extent, and the treeline shifts northwards, almost

CPD

11, 2239–2279, 2015

Climate–vegetation modelling and fossil plant data suggest low atmospheric CO₂ in the late Miocene

M. Forrest et al.

Title Page

Abstract

Introduction

Conclusions

References

Tables

Figures

◀

▶

◀

▶

Back

Close

Full Screen / Esc

Printer-friendly Version

Interactive Discussion



Climate–vegetation modelling and fossil plant data suggest low atmospheric CO₂ in the late Miocene

M. Forrest et al.

[Title Page](#)

[Abstract](#)

[Introduction](#)

[Conclusions](#)

[References](#)

[Tables](#)

[Figures](#)

[◀](#)

[▶](#)

[◀](#)

[▶](#)

[Back](#)

[Close](#)

[Full Screen / Esc](#)

[Printer-friendly Version](#)

[Interactive Discussion](#)



completely replacing tundra in the higher latitudes. In similar fashion, evergreen trees dominate larger areas than deciduous trees in the temperate coastal forests, which may also be linked to the seasonality and humidity changes mentioned above.

In the Southwest and near the Gulf of Mexico, the results are similar in 280 and 450 ppm runs. In the Southwest and south of North America, both simulations produce dry and open vegetation that is similar to the present day (Fig. 1a and b). The runs indicate xeric woodlands and shrublands, dominated by temperate evergreen trees. Further north, these biomes transition to temperate deciduous forests along the Eastern Seaboard, which is in broad agreement with the proxy-based results obtained from the Pacific coastal sites between 35 and 45° N. The main difference between the 280 and 450 ppm runs is that the transitions occur further north in the 450 ppm simulation.

Compared to Pound et al. (2011), in North America our 280 ppm run produces much more open vegetation in the Great Plains, whereas Pound et al. (2011) find more forests. In addition, Pound et al. (2011) reconstruct a large band of temperate grasslands that replaces northern temperate and boreal forests. This is also seen in their Asian reconstruction at similar latitudes, but is not seen in any other reconstruction.

Our model results are fairly consistent with the François et al. (2006) CARAIB model results (their 280 ppm standard Tortonian run). The main differences from our results in North America are that we produce much more open vegetation with 280 ppm CO₂, and much of their eastern forests are tropical seasonal forests, indicating warmer climate. The low CO₂ run of François et al. (with 200 ppm), on the other hand, produced temperate mixed forests in much of North America, with only western North America being more open.

4.3.3 Asia

In Asia, the expected northward biome shifts in the boreal/temperate zone is observed in the 450 ppm simulation relative to the 280 ppm simulation. In a similar fashion to North America and Europe, the temperate-boreal boundary and treelines are at higher latitudes with higher CO₂, resulting in a larger area of temperate deciduous forest, and

Climate–vegetation modelling and fossil plant data suggest low atmospheric CO₂ in the late Miocene

M. Forrest et al.

Title Page

Abstract

Introduction

Conclusions

References

Tables

Figures



Back

Close

Full Screen / Esc

Printer-friendly Version

Interactive Discussion

almost no tundra or boreal deciduous forest, in the 450 ppm simulation (Fig. 1a and b). The 280 ppm biome boundaries are approximately similar to the present day, with the exception that the temperate deciduous forest encroaches much further from Europe into Asia. The only three proxy data points in boreal Asia (Kamchatka, sites Bayokov H1172, Nekkeiveem H3658, Yanran H3690; mixed broadleaved deciduous-conifer forest and mixed shrubland; cf. Popova et al., 2013) indicate that the 280 ppm run fits slightly better (Fig. S2).

Both simulations exhibit a large grass-dominated steppe in Central Asia, but the landscape is not as open as in the present day vegetation. This grass steppe is larger in the 280 ppm run than in the 450 ppm run, and extends slightly further northwards in the western part (Fig. 1a and b). The small difference in aridity and openness in the Asian continental interior between the CO₂ concentration scenarios is much less compared to North America. The few inland proxy points in Central Asia (sites Dunhuang, Kuga Xinjiang, S Junggar, Xining Minhe Basin) all have significantly raised proportions of C₃ grass component, and indicate reasonable agreement, with no difference between the different CO₂ simulations, though a considerable broadleaved arboreal diversity in the proxy data points to more forested conditions when compared to the model. The coastal points at similar latitude on the East China Sea show better agreement with the 280 ppm run (Fig. 1a and b). The 280 ppm run shows more temperate broadleaved evergreen trees in southern and eastern China and the surrounding area, than in the 450 ppm run. Consequently, better agreement index scores are present in the 280 ppm run.

There are few differences between the 280 and 450 ppm simulations in Southwest Asia, South Asia and Southeast Asia; both produce grasslands in the western areas and savanna in east. The savanna transitions to tropical forests in the southeast Asia. However, the 280 ppm run produces dryer grasslands in the west, and slightly fewer trees in the east. Furthermore, the evergreen tropical forest of the 280 ppm scenario (and in present day simulations) is replaced by tropical seasonal and tropical deciduous forests in the 450 ppm scenario. This is unexpected and observed in the 450 ppm

Climate–vegetation modelling and fossil plant data suggest low atmospheric CO₂ in the late Miocene

M. Forrest et al.

Title Page

Abstract

Introduction

Conclusions

References

Tables

Figures

◀

▶

◀

▶

Back

Close

Full Screen / Esc

Printer-friendly Version

Interactive Discussion

day simulation. Their Tortonian simulation also produces a band of savanna along the north east coast, and elements of temperate forest to the south. These forests are not as widespread as in the proxy data, resulting in large corrections in this area. This is mirrored in our results, as the 450 ppm run, with its larger quantity of temperate trees, agrees slightly better with the limited proxy data available in the South (Fig. 1a and b).

The François et al. (2006) 280 ppm model produces grasslands over much of Australia with higher CO₂, and semi-desert and desert with lower CO₂. It also show a band of tropical seasonal forest vegetation along the northeastern coast which extends considerably further inland at higher CO₂ concentrations. On a general level, all the models produce arid biomes over much of Australia, but their exact distributions differ substantially. This may be due to the different representation of xeric vegetation, particularly hbrubs, and due to differences in the classification of biomes, particularly shrublands.

5 Summary and conclusions

We simulated Tortonian vegetation under two plausible atmospheric CO₂ concentrations, using a dynamic global vegetation model forced by AOGCM-based palaeoclimate simulations. We applied a novel approach for comparing modelled vegetation with palaeobotanical data. This approach allowed us to quantitatively test which CO₂ scenario agreed better with the proxy data.

Our results show that the agreement between modelled vegetation and palaeobotanical data is consistently (i.e. overall and in each world region) higher for the 280 ppm model run compared to the 450 ppm run. In other words, the CO₂ level needs to be moderately low in order to maintain the seasonal and open landscapes that are the hallmarks of Late Miocene environments. This strongly suggests that atmospheric CO₂ levels were relatively low during the Late Miocene.

The results are most striking for Central Europe and for Central and West America. The 280 ppm run produces deciduous forests in Central Europe and open landscapes in Southern Europe, in agreement with the palaeobotanical evidence, whereas

Climate–vegetation modelling and fossil plant data suggest low atmospheric CO₂ in the late Miocene

M. Forrest et al.

Title Page

Abstract

Introduction

Conclusions

References

Tables

Figures

◀

▶

◀

▶

Back

Close

Full Screen / Esc

Printer-friendly Version

Interactive Discussion

the 450 ppm run produces more evergreen forests. Similar differences in openness in Central and Western North America occur in the simulations. Due to the scarcity of palaeobotanical data in most of North America, higher AI values cannot be observed for the 280 ppm run. However, the open landscapes observed in the 280 ppm run are supported by multiple lines of evidence, including fossil mammal data, isotopes, and phytoliths. Results from factorial runs, assuming different CO₂ concentrations in the climate and the vegetation model, suggest that climatic effect of CO₂ are most important. Physiological CO₂ effects also play a secondary role, in particular in Central and Western North America. In the continental interior of East Asia there is a small difference in aridity and openness between the two CO₂ concentration scenarios. The few proxy data available inland and in coastal areas along the East China Sea also show better agreement with the 280 ppm run.

We conclude that the Late Miocene vegetation in conjunction with vegetation/climate modeling can be used to constrain CO₂ concentrations in the atmosphere. Further studies shall test this idea using marine data in connection with marine ecosystem models.

Appendix A: Plant Functional Types (PFTs)

The PFTs used follow from Ahlström et al. (2012) with some modifications as noted in the main text. In particular, the parameters for shade-tolerance classes, leaf forms, and growth types are unchanged from Ahlström et al. (2012, Table S2). Table S1 gives a complete list of the PFTs and their parameters, as used in this study.

Appendix B: Biome classification

The biome classification is based on the classification used in Hickler et al. (2006) but includes the modifications used in Smith et al. (2014). It is further modified because the shade intolerant broad-leaved summergreen (IBS) PFT in Smith et al. (2014) has

been split into a temperate shade intolerant broad-leaved summergreen (TeBS) PFT and a boreal shade intolerant broad-leaved summergreen (BBS) PFT for this study. In this classification BBS is treated as BS for classifying boreal forests, and TeBS is added to TeBS when classifying temperature forests.

The Supplement related to this article is available online at doi:10.5194/cpd-11-2239-2015-supplement.

Acknowledgements. J. T. Eronen was supported by A. v Humboldt foundation grant and a Marie Curie fellowship (FP7-PEOPLE-2012-IEF, grant number 329645, to J. T. Eronen and T. Hickler). M. Forrest and T. Hickler acknowledge support through the LOEWE funding program (Landes-Offensive zur Entwicklung wissenschaftlich-ökonomischer Exzellenz) of Hesse's Ministry of Higher Education, Research, and the Arts. T. Utescher thanks the German Science Foundation for the funding obtained (MI 926/8-1). This study is a contribution to *NECLIME* (Neogene Climate Evolution of Eurasia). G. Knorr and C. Stepanek acknowledge funding by the "Helmholtz Climate Initiative REKLIM" (Regional Climate Change), a joint research project of the Helmholtz Association of German research centres.

References

- Agusti, J., Sanz de Siria, A., and Garcés, M.: Explaining the end of the hominoid experiment in Europe, *J. Human Evol.*, 45, 145–153, 2003.
- Ahlström, A., Schurgers, G., Arneeth, A., and Smith, B.: Robustness and uncertainty in terrestrial ecosystem carbon response to CMIP5 climate change projections, *Environ. Res. Lett.*, 7, 044008, doi:10.1088/1748-9326/7/4/044008, 2012.
- Beerling, D. J. and Royer, D. L.: Convergent Cenozoic CO₂ history, *Nat. Geosci.*, 4, 418–20, 2011.
- Bolton, C. T. and Stoll, H. M.: Late Miocene threshold response of marine algae to carbon dioxide limitation, *Nature*, 500, 558–562, 2013.
- Bugmann, H.: A review of forest gap models, *Climatic Change*, 51, 259–305, 2001.
- Ehleringer, J. R., Cerling, T. E., and Helliker, B. R.: C₄ photosynthesis, atmospheric CO₂, and climate, *Oecologia*, 112, 285–299, 1997.

Climate–vegetation modelling and fossil plant data suggest low atmospheric CO₂ in the late Miocene

M. Forrest et al.

Title Page

Abstract

Introduction

Conclusions

References

Tables

Figures

◀

▶

◀

▶

Back

Close

Full Screen / Esc

Printer-friendly Version

Interactive Discussion



**Climate–vegetation
modelling and fossil
plant data suggest
low atmospheric CO₂
in the late Miocene**

M. Forrest et al.

[Title Page](#)[Abstract](#)[Introduction](#)[Conclusions](#)[References](#)[Tables](#)[Figures](#)[◀](#)[▶](#)[◀](#)[▶](#)[Back](#)[Close](#)[Full Screen / Esc](#)[Printer-friendly Version](#)[Interactive Discussion](#)

- Eronen, J. T., Puolamäki, K., Liu, L., Lintulaakso, K., Damuth, J., Janis, C., and Fortelius, M.: Precipitation and large herbivorous mammals, part II: Application to fossil data, *Evol. Ecol. Res.*, 12, 235–248, 2010.
- Eronen, J. T., Fortelius, M., Micheels, A., Portmann, F. T., Puolamäki, K., and Janis, C. M.: Neogene aridification of the Northern Hemisphere, *Geology*, 40, 823–826, 2012.
- Fortelius, M., Eronen, J. T., Kaya, F., Tang, H., Raia, P., and Puolamäki, K.: Evolution of neogene mammals in Eurasia: environmental forcing and biotic interactions, *Annu. Rev. Earth Pl. Sc.*, 42, 579–604, 2014.
- Foster, G. L., Lear, C. H., and Rae, J. W. B.: The evolution of $p\text{CO}_2$, ice volume and climate during the middle Miocene, *Earth Planet. Sc. Lett.*, 341–344, 243–254, 2012.
- François, L., Ghislain, M., Otto, D., and Micheels, A.: Late Miocene vegetation reconstruction with the CARAIB model, *Palaeogeogr. Palaeoclimatol.*, 238, 302–320, 2006.
- François, L., Utescher, T., Favre, E., Henrot, A. J., Warnant, P., Micheels, A., Erdei, B., Suc, J. P., Cheddadi, R., and Mosbrugger, V.: Modelling Late Miocene vegetation in Europe: results of the CARAIB model and comparison with palaeovegetation data, *Palaeogeogr. Palaeoclimatol.*, 304, 359–378, 2011.
- François, L. M., Delire, C., Warnant, P., and Munhoven, G.: Modelling the glacial–interglacial changes in the continental biosphere, *Global Planet. Change*, 16, 37–52, 1998.
- Gerten, D., Schaphoff, S., Haberlandt, U., Lucht, W., and Sitch, S.: Terrestrial vegetation and water balance – hydrological evaluation of a dynamic global vegetation model, *J. Hydrol.*, 286, 249–270, 2004.
- Gradstein, F. M., Ogg, J. G., Smith, A. G., Agterberg, F. P., Bleeker, W., Cooper, R. A., Davydov, V., Gibbard, P., Hinnov, L. A., House, M. R. (†), Lourens, L., Luterbacher, H.-P., McArthur, J., Melchin, M. J., Robb, L. J., Sadler, P. M., Shergold, J., Villeneuve, M., Wardlaw, B. R., Ali, J., Brinkhuis, H., Hilgen, F. J., Hooker, J., Howarth, R. J., Knoll, A. H., Laskar, J., Monechi, S., Powell, J., Plumb, K. A., Raffi, I., Röhl, U., Sanfilippo, A., Schmitz, B., Shackleton, N. J., Shields, G. A., Strauss, H., Van Dam, J., Veizer, J., Van Kolschoten, T., and Wilson, D.: *Geologic Time Scale 2004*, Cambridge University Press, Cambridge, UK, 2004.
- Harrison, S. and Prentice, C. I.: Climate and CO₂ controls on global vegetation distribution at the last glacial maximum: analysis based on paleovegetation data, biome modelling and paleoclimate simulations, *Glob. Change Biol.*, 9, 983–1004, 2003.

**Climate–vegetation
modelling and fossil
plant data suggest
low atmospheric CO₂
in the late Miocene**

M. Forrest et al.

[Title Page](#)[Abstract](#)[Introduction](#)[Conclusions](#)[References](#)[Tables](#)[Figures](#)[◀](#)[▶](#)[◀](#)[▶](#)[Back](#)[Close](#)[Full Screen / Esc](#)[Printer-friendly Version](#)[Interactive Discussion](#)

Haxeltine, A. and Prentice, I. C.: BIOME3: an equilibrium terrestrial biosphere model based on ecophysiological constraints, resource availability, and competition among plant functional types, *Global Biogeochem. Cy.*, 10, 693–709, 1996.

Hickler, T., Smith, B., Sykes, M. T., Davis, M. B., Sugita, S., and Walker, K.: Using a generalized vegetation model to simulate vegetation dynamics in northeastern USA, *Ecology*, 85, 519–530, 2004.

Hickler, T., Prentice, I. C., Smith, B., Sykes, M. T., and Zaehle, S.: Implementing plant hydraulic architecture within the LPJ Dynamic Global Vegetation Model, *Global Ecol. Biogeogr.*, 15, 567–577, 2006.

Hickler, T., Vohland, K., Feehan, J., Miller, P. A., Smith, B., Costa, L., Giesecke, T., Fronzek, S., Carter, T. R., Cramer, W., Kühn, I., and Sykes, M. T.: Projecting the future distribution of European potential natural vegetation zones with a generalized, tree speciesbased dynamic vegetation model, *Global Ecol. Biogeogr.*, 21, 50–63, 2012.

Herold, N., Seton, M., Müller, R. D., You, Y., and Huber, M.: Middle Miocene tectonic boundary conditions for use in climate models. *Geochem. Geophys. Geos.*, 9, Q10009, doi:10.1029/2008GC002046, 2008.

Janis, C. M., Damuth, J., and Theodor, J. M.: The origins and evolution of the North American grassland biome: the story from the hoofed mammals, *Palaeogeogr. Palaeoclimatol.*, 177, 183–198, 2002.

Janis, C. M., Damuth, J., and Theodor, J. M.: The species richness of Miocene browsers, and implications for habitat type and primary productivity in the North American grassland biome, *Palaeogeogr. Palaeoclimatol.*, 207, 371–398, 2004.

Kaplan, J. O.: Geophysical applications of vegetation modeling, No. ARVE-THESIS-2009-001, Lund University, Lund, Sweden, 2001.

Knorr, G. and Lohmann, G.: Climate warming during Antarctic ice sheet expansion at the Middle Miocene transition, *Nat. Geosci.*, 7, 376–381, 2014.

Knorr, G., Butzin, M., Micheels, A., and Lohmann, G.: A warm Miocene climate at low atmospheric CO₂ levels, *Geophys. Res. Lett.*, 38, L20701, doi:10.1029/2011GL048873, 2011.

Kürshner, W. M., Kvacek, Z., and Dilcher, D. L.: The impact of Miocene atmospheric carbon dioxide fluctuations on climate and the evolution of terrestrial ecosystems, *P. Natl. Acad. Sci. USA*, 105, 449–453, 2008.

Climate–vegetation modelling and fossil plant data suggest low atmospheric CO₂ in the late Miocene

M. Forrest et al.

[Title Page](#)

[Abstract](#)

[Introduction](#)

[Conclusions](#)

[References](#)

[Tables](#)

[Figures](#)

[◀](#)

[▶](#)

[◀](#)

[▶](#)

[Back](#)

[Close](#)

[Full Screen / Esc](#)

[Printer-friendly Version](#)

[Interactive Discussion](#)



LaRiviere, J. P., Ravelo, A. C., Crimmins, A., Dekens, P. S., Ford, H. L., Lyle, M., and Wara, M. W.: Late Miocene decoupling of oceanic warmth and atmospheric carbon dioxide forcing, *Nature*, 486, 97–100, 2012.

Lavigne, M. B. and Ryan, M. G.: Growth and maintenance respiration rates of aspen, black spruce and jack pine stems at northern and southern BOREAS sites, *Tree Physiol.*, 17, 543–551, 1997.

Lyle, M., Barron, J., Bralower, T. J., Huber, M., Olivares Lyle, A., Ravelo, A. C., Rea, D. K., and Wilson, P. A.: Pacific Ocean and Cenozoic evolution of climate, *Rev. Geophys.*, 46, RG2002/2008, doi:10.1029/2005RG000190, 2008.

Marsland, S. J., Haak, H., Jungclaus, J. H., Latif, M., and Röske, F.: The Max-Planck-Institute global ocean/sea ice model with orthogonal curvilinear coordinates, *Ocean Model.*, 5, 91–127, 2003.

Micheels, A.: Late Miocene climate modelling with echam4/ml – the effects of the palaeovegetation on the Tortonian climate, unpublished thesis, Eberhard-Karls Universität Tübingen, 2003.

Micheels, A., Bruch, A. A., Uhl, D., Utescher, T., and Mosbrugger, V.: A late Miocene climate model simulation with ECHAM4/ML and its quantitative validation with terrestrial proxy data, *Palaeogeogr. Palaeoclimatol.*, 253, 251–270, 2007.

Micheels, A., Bruch, A. A., Eronen, J., Fortelius, M., Harzhauser, M., Utescher, T., and Mosbrugger, V.: Analysis of heat transport mechanisms from a Late Miocene model experiment with a fully-coupled atmosphere–ocean general circulation model, *Palaeogeogr. Palaeoclimatol.*, 304, 337–50, 2011.

Morgan, J. A., Milchunas, D. G., LeCain, D. R., West, M., and Mosier, A. R.: Carbon dioxide enrichment alters plant community structure and accelerates shrub growth in the shortgrass steppe, *P. Natl. Acad. Sci. USA*, 37, 14724–14729, 2007.

Mosbrugger, V., Utescher, T., and Dilcher, D. L.: Cenozoic continental climatic evolution of Central Europe, *P. Natl. Acad. Sci. USA*, 102, 14964–14969, 2005.

Pachzelt, A., Forrest, M., Rammig, A., Higgins, S., and Hickler, T.: Potential impact of large ungulate grazers on African vegetation, carbon storage and fire regimes, *Global Ecol. Biogeogr.*, doi:10.1111/geb.12313, online first, 2015.

Passey, B. H., Cerling, T. E., Perkins, M. E., Voorhies, M. R., Harris, J. M., and Tucker, S. T.: Environmental change in the Great Plains: an isotopic record from fossil horses, *J. Geol.*, 110, 123–140, 2002.

Climate–vegetation modelling and fossil plant data suggest low atmospheric CO₂ in the late Miocene

M. Forrest et al.

[Title Page](#)
[Abstract](#)
[Introduction](#)
[Conclusions](#)
[References](#)
[Tables](#)
[Figures](#)




[Back](#)
[Close](#)
[Full Screen / Esc](#)
[Printer-friendly Version](#)
[Interactive Discussion](#)

dynamic vegetation model, *Biogeosciences*, 11, 2027–2054, doi:10.5194/bg-11-2027-2014, 2014.

Stephuhn, A., Micheels, A., Geiger, G., and Mosbrugger, V.: Reconstructing the Late Miocene climate and oceanic heat flux using the AGCM ECHAM4 coupled to a mixed-layer ocean model with adjusted flux correction, *Palaeogeogr. Palaeoclimatol.*, 238, 399–423, 2006.

Steininger, F. F.: Chronostratigraphy, geochronology and biochronology of the Miocene European Land Mammal Mega-Zones (ELMMZ) and the Miocene mammal-zones, in: *The Miocene Land Mammals of Europe*, Verlag Dr. Friedrich Pfeil, Munich, Germany, 9–24, 1999.

Stewart, D. R. M., Pearson, P. N., Ditchfield, P. W., and Singano, J. M.: Miocene tropical Indian Ocean temperatures: evidence from three exceptionally preserved foraminiferal assemblages from Tanzania, *J. Afr. Earth Sci.*, 40, 173–190, 2004.

Strömberg, C. A. E.: Decoupled taxonomic radiation and ecological expansion of open-habitat grasses in the Cenozoic of North America, *P. Natl. Acad. Sci. USA*, 102, 11980–11984, 2005.

Strömberg C. A. E.: Evolution of grasses and grassland ecosystems, *Annu. Rev. Earth Pl. Sc.*, 39, 517–544, 2011.

Syabryaj, S., Molchanoff, S., Utescher, T., and Bruch, A. A.: Changes of climate and vegetation during the Miocene on the territory of Ukraine, *Palaeogeogr. Palaeoclimatol.*, 253, 153–168, 2007.

Thonicke, K., Venevsky, S., Sitch, S., and Cramer, W.: The role of fire disturbance for global vegetation dynamics: coupling fire into a Dynamic Global Vegetation Model, *Global Ecol. Biogeogr.*, 10, 661–677, 2001.

Utescher, T., Erdei, B., Francois, L., and Mosbrugger, V.: Tree diversity in the Miocene forests of Western Eurasia, *Palaeogeogr. Palaeoclimatol.*, 253, 242–266, 2007.

Utescher, T., Bruch, A. A., Micheels, A., Mosbrugger, V., and Popova, S.: Cenozoic climate gradients in Eurasia – a palaeo-perspective on future climate change?, *Palaeogeogr. Palaeoclimatol.*, 304, 351–358, 2011.

Williams, M., Haywood, A. M., Taylor, S. P., Valdes, P. J., Sellwood, B. W., and Hillenbrand, C. D.: Evaluating the efficacy of planktonic foraminifer calcite delta ¹⁸O data for sea surface temperature reconstruction for the Late Miocene, *Geobios*, 38, 843–863, 2005.

Wolfe, J. A.: Tertiary climatic changes at middle latitudes of western North America, *Palaeogeogr. Palaeoclimatol.*, 108, 195–205, 1994a.

Wolfe, J. A.: An analysis of Neogene climates in Beringia, *Palaeogeogr. Palaeoclimatol.*, 108, 207–216, 1994b.

CPD

11, 2239–2279, 2015

Climate–vegetation modelling and fossil plant data suggest low atmospheric CO₂ in the late Miocene

M. Forrest et al.

Title Page

Abstract

Introduction

Conclusions

References

Tables

Figures



Back

Close

Full Screen / Esc

Printer-friendly Version

Interactive Discussion

Climate–vegetation modelling and fossil plant data suggest low atmospheric CO₂ in the late Miocene

M. Forrest et al.

[Title Page](#)

[Abstract](#)

[Introduction](#)

[Conclusions](#)

[References](#)

[Tables](#)

[Figures](#)



[Back](#)

[Close](#)

[Full Screen / Esc](#)

[Printer-friendly Version](#)

[Interactive Discussion](#)



Table 1. Contributions to the Agreement Index for each combination of data and model statuses.

		MODEL			
		Absent	Trace	Sub-dominant	Dominant
DATA	Absent	0	0	−1	−2
	Trace	0	1	0	−1
	Sub-dominant	−1	0	1	0
	Dominant	−2	−1	0	2

Climate–vegetation modelling and fossil plant data suggest low atmospheric CO₂ in the late Miocene

M. Forrest et al.

[Title Page](#)

[Abstract](#)

[Introduction](#)

[Conclusions](#)

[References](#)

[Tables](#)

[Figures](#)

⏪

⏩

◀

▶

[Back](#)

[Close](#)

[Full Screen / Esc](#)

[Printer-friendly Version](#)

[Interactive Discussion](#)



Table 2. Global Agreement Index values from all permutations of 280 and 450 ppm CO₂ concentrations in the climate and vegetation models.

		Vegetation CO ₂	
		280 ppm	450 ppm
Climate CO ₂	280 ppm	−0.67	−0.60
	450 ppm	−1.02	−0.96

Climate–vegetation modelling and fossil plant data suggest low atmospheric CO₂ in the late Miocene

M. Forrest et al.

[Title Page](#)

[Abstract](#)

[Introduction](#)

[Conclusions](#)

[References](#)

[Tables](#)

[Figures](#)



[Back](#)

[Close](#)

[Full Screen / Esc](#)

[Printer-friendly Version](#)

[Interactive Discussion](#)



Table 3. Central European Agreement Index values from all permutations of 280 and 450 ppm CO₂ concentrations in the climate and vegetation models. For these purposes, Central Europe is defined to lie in the longitude range [0, 25] and latitude range [45, 50].

		Vegetation CO ₂	
		280 ppm	450 ppm
Climate CO ₂	280 ppm	0.17	0.19
	450 ppm	0.01	−0.03

Climate–vegetation modelling and fossil plant data suggest low atmospheric CO₂ in the late Miocene

M. Forrest et al.

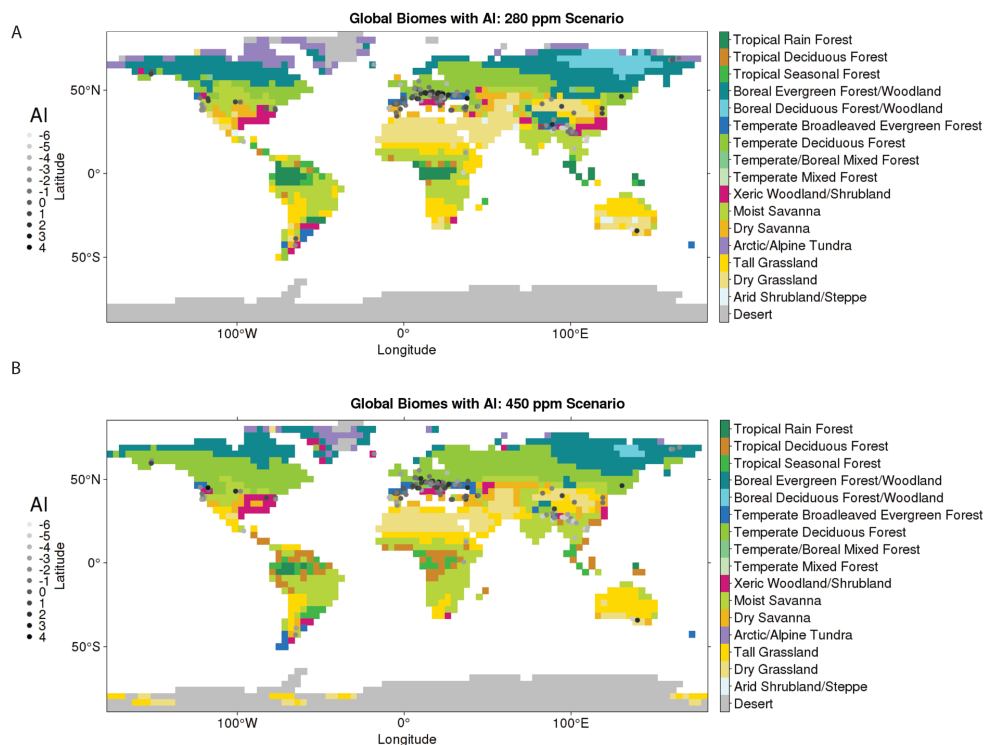


Figure 1. Modelled Late Miocene (Tortonian, 7–11 Ma) vegetation, using the ECHAM5-MPIOM AOGCM to drive LPJ-GUESS. **(a)** The biome distribution with 280 ppm CO₂ concentration, with the Agreement Index (AI) match overlay for palaeobotanical data. **(b)** The biome distribution with 450 ppm CO₂ concentration, with the AI match overlay for palaeobotanical data. **(c)** The dominant PFTs, with palaeobotanical data classified with same PFT scheme as the model overlay, with 280 ppm CO₂ concentration. **(d)** The dominant PFTs, with palaeobotanical data classified with same PFT scheme as the model overlay, with 450 ppm CO₂ concentration.

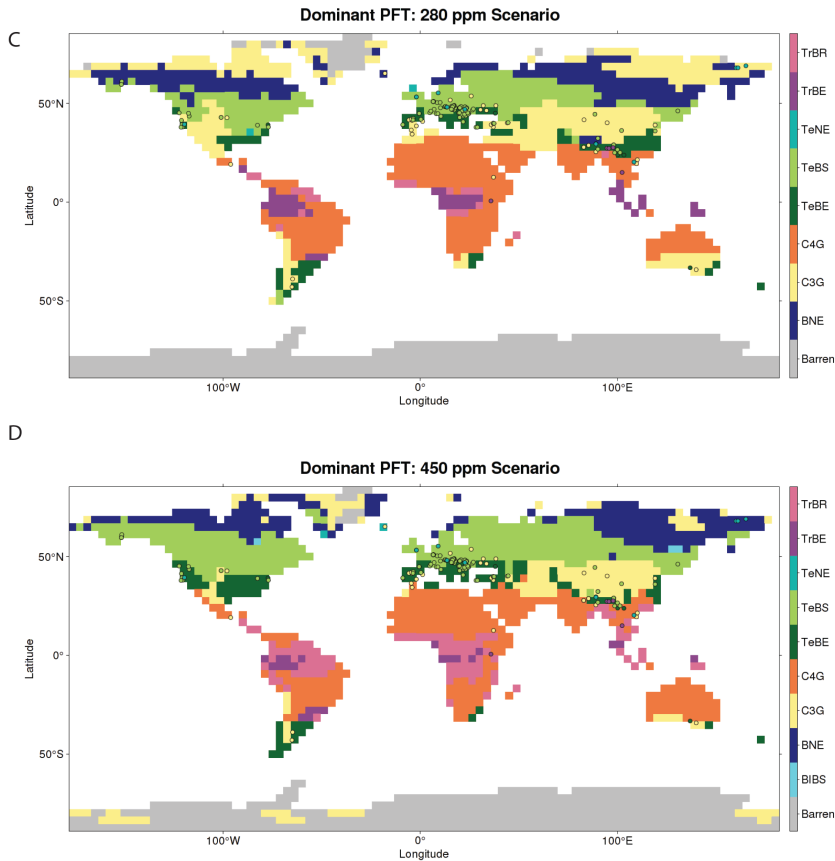


Figure 1. Continued.

Climate–vegetation modelling and fossil plant data suggest low atmospheric CO₂ in the late Miocene

M. Forrest et al.

[Title Page](#)

[Abstract](#) [Introduction](#)

[Conclusions](#) [References](#)

[Tables](#) [Figures](#)

[◀](#) [▶](#)

[◀](#) [▶](#)

[Back](#) [Close](#)

[Full Screen / Esc](#)

[Printer-friendly Version](#)

[Interactive Discussion](#)



Climate–vegetation modelling and fossil plant data suggest low atmospheric CO₂ in the late Miocene

M. Forrest et al.

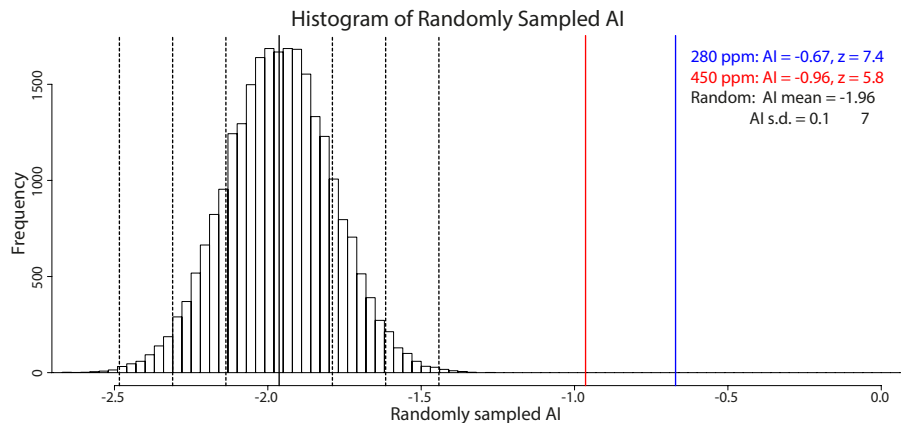


Figure 2. Agreement Index with the null model distribution and the AI values shown for model runs with different CO₂ concentration.

Title Page

Abstract

Introduction

Conclusions

References

Tables

Figures

◀

▶

◀

▶

Back

Close

Full Screen / Esc

Printer-friendly Version

Interactive Discussion

Climate–vegetation modelling and fossil plant data suggest low atmospheric CO₂ in the late Miocene

M. Forrest et al.

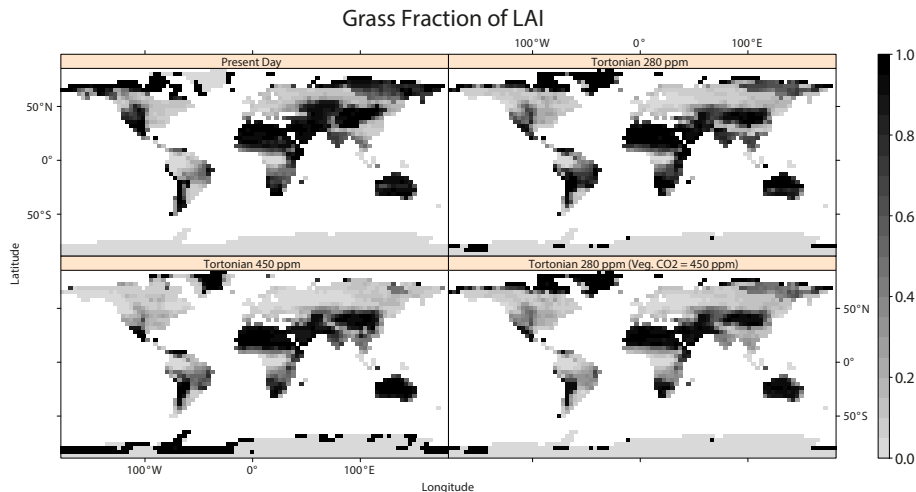


Figure 3. Modelled grass fraction of Leaf Area Index (LAI) for present-day simulation, Tortonian 280 ppm CO₂, and Tortonian 450 ppm CO₂ concentrations, respectively. Shown also is the grass fraction of LAI for a mixed CO₂ forcing in climate and vegetation model.

Title Page

Abstract

Introduction

Conclusions

References

Tables

Figures

◀

▶

◀

▶

Back

Close

Full Screen / Esc

Printer-friendly Version

Interactive Discussion

Climate–vegetation modelling and fossil plant data suggest low atmospheric CO₂ in the late Miocene

M. Forrest et al.

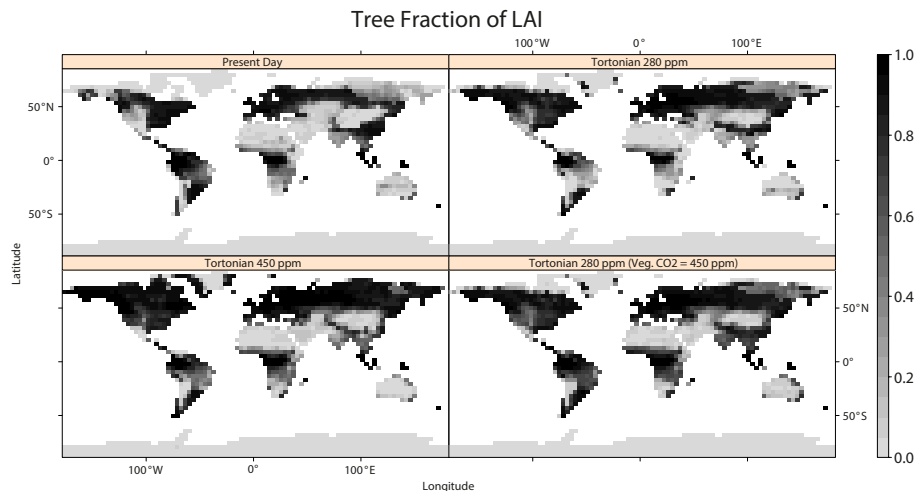


Figure 4. Modelled tree fraction of Leaf Area Index (LAI) for present-day simulation, Tortonian 280 ppm CO₂, and Tortonian 450 ppm CO₂ concentrations, respectively. Shown also is the tree fraction of LAI for a mixed CO₂ forcing in climate and vegetation model.

Title Page

Abstract

Introduction

Conclusions

References

Tables

Figures

◀

▶

◀

▶

Back

Close

Full Screen / Esc

Printer-friendly Version

Interactive Discussion

